Utilizing Visible Light to Enable Contra-Thermodynamic Skeletal Rearrangement for Dearomative *meta*-Cycloadditions of 2-Acetonaphthalenes via Triplet Energy Transfer Cascade

Pramod Rai,[a] Sanghamitra Naik,[a] Kriti Gupta,[b] Garima Jindal,[b,*] Biplab Maji[a,*]

[a]Department of Chemical Sciences, Indian Institute of Science Education and Research Kolkata, Mohanpur 741246, West Bengal, India

[b]Department of Organic Chemistry, Chemical Sciences Division, Indian Institute of Science, Bangalore, Karnataka-560012, India

Email: gjindal@iisc.ac.in, bm@iiserkol.ac.in

Abstract

With the renaissance of visible light-mediated triplet-triplet energy transfer (^{VL}EnT) catalysis as a greener and milder catalytic regime, dearomative cycloadditions (DAC) have emerged as a powerful arsenal in arriving at sophisticated three-dimensional molecular scaffolds. With *ortho*- and *para*-variants having been well documented under ^{VL}EnT catalysis and dearomative *meta*-cycloadditions being known to be symmetry allowed in the excited singlet potential energy surface under harsher UV irradiations, the prospective [3 + 2] dearomative cycloadditions propelled via a ^{VL}EnT catalysis remains elusive. Herein, we report a formal dearomative *meta*-cycloaddition of 2-acetonaphthalenes propagated via a two-step ^{VL}EnT cascade circumventing the attainment of energetically higher singlet excited states. The work showcases the judicious selection of photosensitizer backed by DFT calculations to selectively promote the [4 + 2] DAC followed by a *contra*-thermodynamic stepwise skeleton rearrangement cascade. The detailed DFT studies in conjugation with electrochemical, photoluminescence, kinetic, quadratic dependency, and control experiments support the ^{VL}EnT cascade. The observed *meta*-selectivity over *ortho*- and *para*-DAC was rationalized by the reactivity difference in the singlet and triplet spin surfaces. The described protocol delivers highly sp^3-rich polycyclic frameworks in high yields and moderate selectivities with wide functional group tolerance. The inclusion of bioactive agents and the establishment of a wide array of post-synthetic derivatizations further climaxes the efficiency of the designed protocol.

Introduction

The discovery of protocols for molecules possessing intricate arrays of three-dimensional (3D) rings is typically a long and arduous endeavor.[1-3] Traditionally, this relies on multistep procedures, leading to constraints in terms of time, cost, and environmental impact due to post-reaction treatments after each step. Overcoming these challenges by implementing strategies involving straightforward one-pot sequences or cascades to produce the targeted polycyclic rings is highly desirable.[4-6]

Dearomative cycloaddition (DAC) reactions are acknowledged for their capacity to rapidly and efficiently generate molecular complexity,[7, 8] creating sp^3-enriched 3D complex molecules from simple 2D aromatic feedstocks.[9-12] The advanced study of DAC chemistry encompasses the topological possibilities of introducing new C-C bonds in [2 + 2] (*ortho*),[13-24] [3 + 2] (*meta*),[25, 26] or [4 + 2] (*para*)[27-35] fashions to aromatic precursors, thus allowing access to various complex frameworks that would otherwise be difficult to synthesize via conventional pathways (Figure 1a).

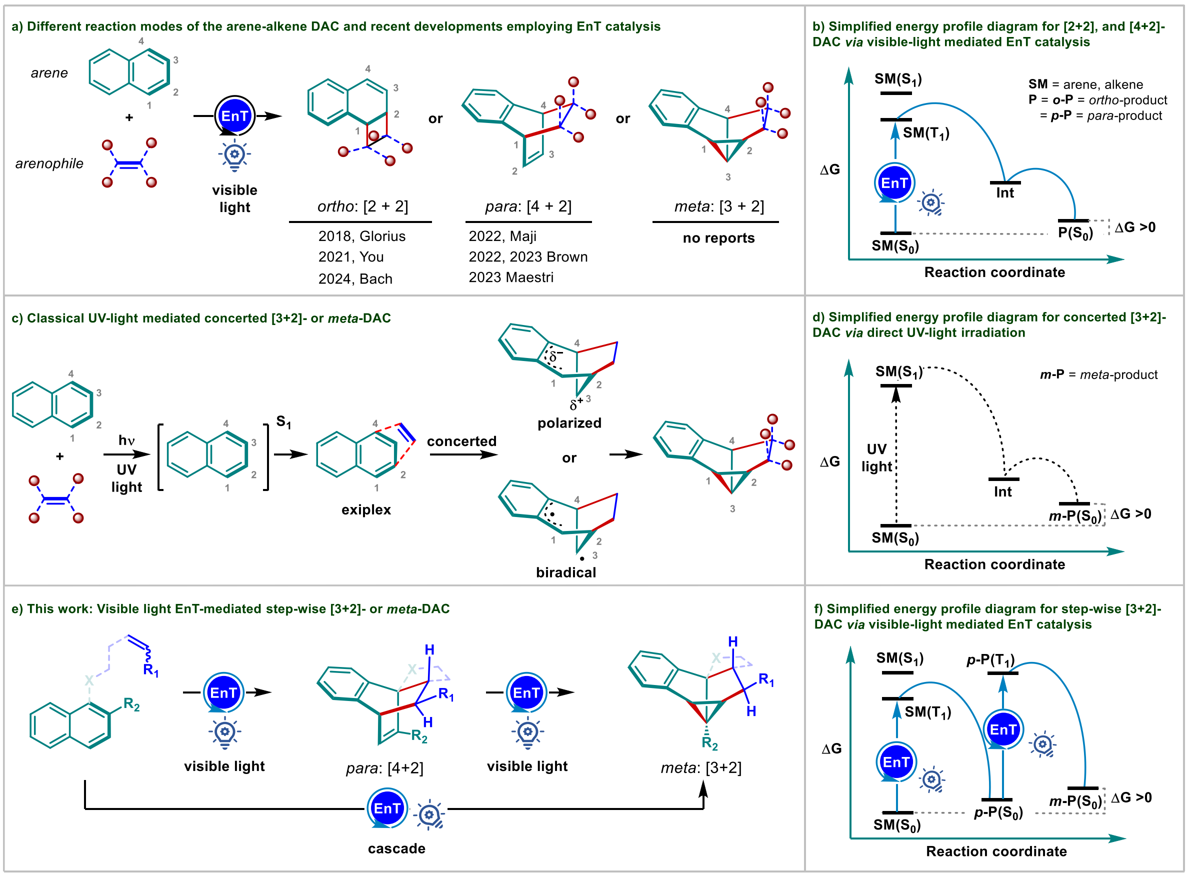

Figure 1: (a) Different Reaction Modes of the Arene-Alkene Dearomative Cycloaddition and Recent Developments Employing EnT Catalysis, and (b) their Simplified Reaction Profile; (c) Classical UV Light-Mediated Concerted [3+2]- or *meta*-DAC, and (d) its Simplified Reaction Profile; (e) This work: Visible Light EnT-Mediated Stepwise [3+2]- or *meta*-DAC, and (f) its Simplified Reaction Profile.

Although the expected product diversity can serve as an ideal clickbait to explore the 3D chemical space, controlling the selectivity still remains a fundamental challenge.[36, 37] Furthermore, classical photochemical DAC reactions employ ultraviolet (UV) light to drive the reaction by accessing the excited potential energy surface, negating the high barrier and the microscopic reversibility observed in thermal ground state reactivity.[38] The use of highly energetic harmful UV irradiation in these maneuvers lowers the probability of achieving the desired selectivity and constrains their widespread use from a synthetic viewpoint.

Recently, visible light-mediated triplet-triplet energy transfer (^{VL}EnT) catalysis has emerged as a powerful tool to initiate DACs (Figures 1a, b).[20, 39-42] The underlying concept is circumferent to achieving the excited triplet state population via EnT from an appropriate photosensitizer (PS) to the substrate. This approach leverages the enormous potential of excited state reactivity by employing mild visible light energy while ensuring the desired selectivity. The discovery of an impressive portfolio of PSs with a broad range of triplet energies (E_T) facilitates visible light photosensitized DACs of various flat aromatic substrates to form sp^3-rich polycyclic architectures with diverse applications. Prominent examples of ^{VL}EnT-mediated dearomative [2 + 2] and [4 + 2] cycloaddition reactions of (hetero)aromatic compounds, with both intra- and intermolecular versions can be found in the recent elegant works of You, Glorius, Brown, König, Bach, Schindler, Maestri, Fu, Nolan, Morofuji, Guin, and others (Figure 1a).[13-24, 27-35, 43-45] We also took an interest in developing dearomative photocycloadditions of simple polycyclic aromatic hydrocarbon naphthalene motifs.[34] Nevertheless, despite the significant advancements in this field, as far as our knowledge extends, the ^{VL}EnT-mediated dearomative [3 + 2] or *meta* cycloaddition (*meta*-DAC) reactions have not been reported yet (Figure 1a).

We were recently intrigued by the possibility of achieving the [3 + 2]- or *meta*-DAC of 2-acetonaphthalenes under ^{VL}EnT catalysis. Classically, *meta*-DAC is symmetry allowed in the first excited singlet potential energy surface under UV light irradiation *via* the formation of an exciplex with the alkene, and the two σ-bonds are formed in a concerted manner as pictorially represented in Figures 1c, d.[46, 47] We anticipate that a formal *meta*-cycloadduct could potentially be obtained through a two-step ^{VL}EnT cascade, all without the need to access the singlet excited state (Figures 1e,f). More specifically, we envision engaging naphthalene and alkene in a stepwise EnT-mediated *para*-cycloaddition followed by EnT-mediated rearrangement of the resulting cycloadduct in a cascade manner under visible-light irradiation. However, we have recognized the challenge posed by the endergonic nature of this process. It is anticipated that the initial *para*-cycloaddition that involvs the loss of aromaticity would be thermodynamically demanding. The conversion of the *para*-cycloadduct to the formal *meta*-cycloadduct would further be endergonic primarily due to the enhanced strain in the polycyclic framework. Appropriate choice of PS and reaction conditions would be vital for the success of this *contra*-thermodynamic cascade process.

Result and Discussion

We initiated our experiment with naphthalene-tethered alkene (*Z*)-**1** as the model substrate to establish the intramolecular variant of the reaction (Table 1). From a synthetic perspective, this transformation will deliver highly sp^3-rich polycyclic spiroether scaffolds, which are ubiquitous structural motifs in various bioactive compounds and drugs of natural origins.[48-57] We performed computational studies to determine the E_T ($\Delta G(T_1–S_0)$ = 53.6 kcal/mol) for substrate (*Z*)-**1** (Table S13). It offers valuable guidance for choosing an appropriate photocatalyst among the myriad of available options. Irradiating (*Z*)-**1** in the presence of 4CzIPN (**PS1**, E_T = 53 kcal/mol) in acetonitrile solvent under 427 nm light emitting diode (LED) only produced the *para*-cycloadduct **2** in 64% yield with 3.3:1 *endo*:*exo* ratio (Table 1, entry 1). In comparison, the use of *fac*-Ir(ppy)$_3$ (**PS2**, E_T = 58.1 kcal/mol) as the PS gave a mixture of *para*-cycloadduct **2** and *meta*-cycloadduct **3** in a combined 72% yield with **2**:**3** = 2:1 under the same conditions (entry 2). While the formation of **3** confirmed our mechanistic hypothesis, the lower yield suggested the necessity of PSs with higher E_Ts. The E_T of *endo*-**2** was computed to be 58.6 kcal/mol. Pleasingly, the *meta*-cycloadduct **3** was exclusively isolated in 79% yield with 2.4:1 *endo*:*exo* ratio when the reaction was performed in the presence of [Ir{dF(CF_3)ppy}$_2$(dtbbpy)]PF_6 (**PS3**, E_T = 61.8 kcal/mol, entry 3). Further screening of the reaction parameters identified that the organic PS thioxanthone (**PS4**, E_T = 64.8 kcal/mol) coupled with 405 nm LED irradiation was superior in reactivity and diastereoselectivity, providing the *meta*-cycloadduct **3** in 84% yield and 6:1 *endo*:*exo* ratio (entry 4). However, lower yield and diastereoselectivity were obtained when xanthone (**PS5**, E_T = 74 kcal/mol) was used (entry 5). The structures of the *endo*- and *exo*-isomers were confirmed via single-crystal X-ray diffractrometry.[58] Further details of reaction optimization are tabulated in the Supporting Information section.

The most conspicuous feature of this work is the [3 + 2] selectivity over the [2 + 2] and [4 + 2] cycloadduct generation. The pioneering work of Glorius and recent elegant work by Bach demonstrated that a naphthalene-tethered terminal alkene, when exposed to visible light in the presence of an appropriate photosensitizer, yields a [2 + 2] cycloadduct.[13, 59] You explored the intramolecular [4 + 2], and [4 + 5] cycloadditions of naphthalene-tethered indoles and vinyl cyclopropanes, respectively.[28, 60] We, Brown, and Maestri independently developed the inter- and intra-molecular *para*-DAC of naphthalenes.[29, 34, 35] Control and mechanistic experiments were performed to explore the salient features of the selective *meta*-DAC reaction.

Table 1: Optimization Table.[a]

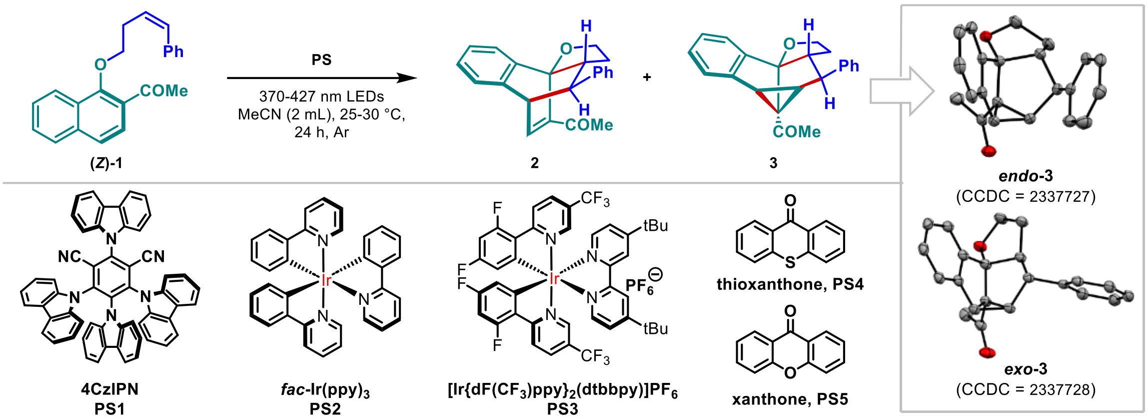

Entry	Photosensitizer (**PS**, mol%, light wavelength)	E_T (kcal/mol)	$E_{1/2}$ (**PS.**)*/(**PS**$^{\bullet-}$) in V vs SCE	$E_{1/2}$ (**PS**$^{\bullet+}$)/(**PS**)* in V vs SCE	% Yield of **2** (*endo*:*exo*)	% Yield of **3** (*endo*:*exo*)
1	**PS1**, 10 mol%, 427 nm	53	+1.49	–1.24	64 (3.3:1)	<5
2	**PS2**, 1 mol%, 427 nm	58.1	+0.31	–1.73	48 (3:1)	24 (3.5:1)
3	**PS3**, 1 mol%, 427 nm	61.8	+1.21	–0.89	<5	79 (2.4:1)
4	**PS4**, 15 mol%, 405 nm	64.8	+1.87	–1.65	<5	84 (6:1)
5	**PS5**, 10 mol%, 370 nm	74	+1.80	–1.65	<5	44 (3.4:1)
Control experiments (deviation from entry 4)						
6	No light				<5	<5
7	No **PS4**				<5	<5
8	(*E*)-**1** is used as a substrate instead of (*Z*)-**1**				<5	65 (3.5:1)
9	in the presence of a triplet quencher: O_2 (1 atm)				<5	<5
10	in the presence of a triplet quencher: 2,5-dimethylhexa-2,4-diene (1 equiv)				<5	<5

[a]Reaction condition: **1** (0.1 mmol), photosensitizer, CH_3CN (2 mL), 370-427 nm LED irradiation under N_2 at 25–30 °C, 24 h. Yield and *endo*:*exo* ratios of **2** and **3** were determined by ^{1}H NMR analysis by using trimethoxy benzene as an internal standard. E_T and $E_{1/2}$ of the **PS** from ref.[34, 61-63]

The experiments conducted without light or **PS4** led to no detection of the cycloadducts **2** and **3**, confirming the necessity of these components in the ^{VL}EnT-mediated cascade reactions (Table 1, entries 6,7). The UV-visible spectrum of **1**, **2**, and **PS4** revealed that only **PS4** absorbs in the visible region of the spectrum emitted by the 405 nm light source (Figure 2a). As shown in Table 1, the yields of the **3** could be allied with the intrinsic E_Ts of the PSs rather than their redox potentials, which suggested the involvement of EnT catalysis. Furthermore, the cyclic voltammetry analysis indicated that an electron transfer from the excited **PS4** ($E_{1/2}$(**PS4**$^{\bullet+}$)/(**PS4**)* = −1.65 V *vs.* saturated calomel electrode (SCE)) to (*Z*)-**1** ($E_{1/2}$ = −1.93 V *vs.* SCE) is thermodynamically endergonic (SI S53). Similarly, an oxidative quenching of the excited **PS4** ($E_{1/2}$(**PS4**)*/(**PS4**$^{\bullet-}$) = 1.87 V *vs.* SCE) could also be ruled out. Additionally, Stern–Volmer analysis revealed an effectual quenching of the photoexcited **PS3**'s luminescence by (*Z*)-**1** (Stern–Volmer quenching constant $k_q = 11.7 \times 10^4$ M^{-1} s^{-1}, Figure 2b). Further, to fathom whether it was the naphthalene ring or the alkene tethered to naphthalene actually responsible for quenching the excited photocatalyst, the quenching experiments were performed with the alkanetethered naphthalene ***sat*-1**. The experiment revealed that ***sat*-1** also interacted with the photoexcited **PS3** efficiently ($k_q = 5.91 \times 10^4\ M^{-1}\ s^{-1}$). These studies disclosed that the excited triplet states of the PSs were more readily quenched by the aromatic ring of the naphthol fragment of **1** than the tethered alkene. Accordingly, the alkene geometry in **1** poised a negligible influence on the reactivity and selectivity (Table 1, entry 8). The (*E*)-**1** also gave product **3** in similar yield and selectivities under these conditions. Furthermore, introducing the well-known triplet state quenchers, such as molecular oxygen and 2,5-dimethylhexa-2,4-diene into the reaction medium resulted in the complete inhibition of the DAC reaction (Table 1, entries 9,10). These agreed with the hypothesis of the EnT process being involved in the catalytic cycle.

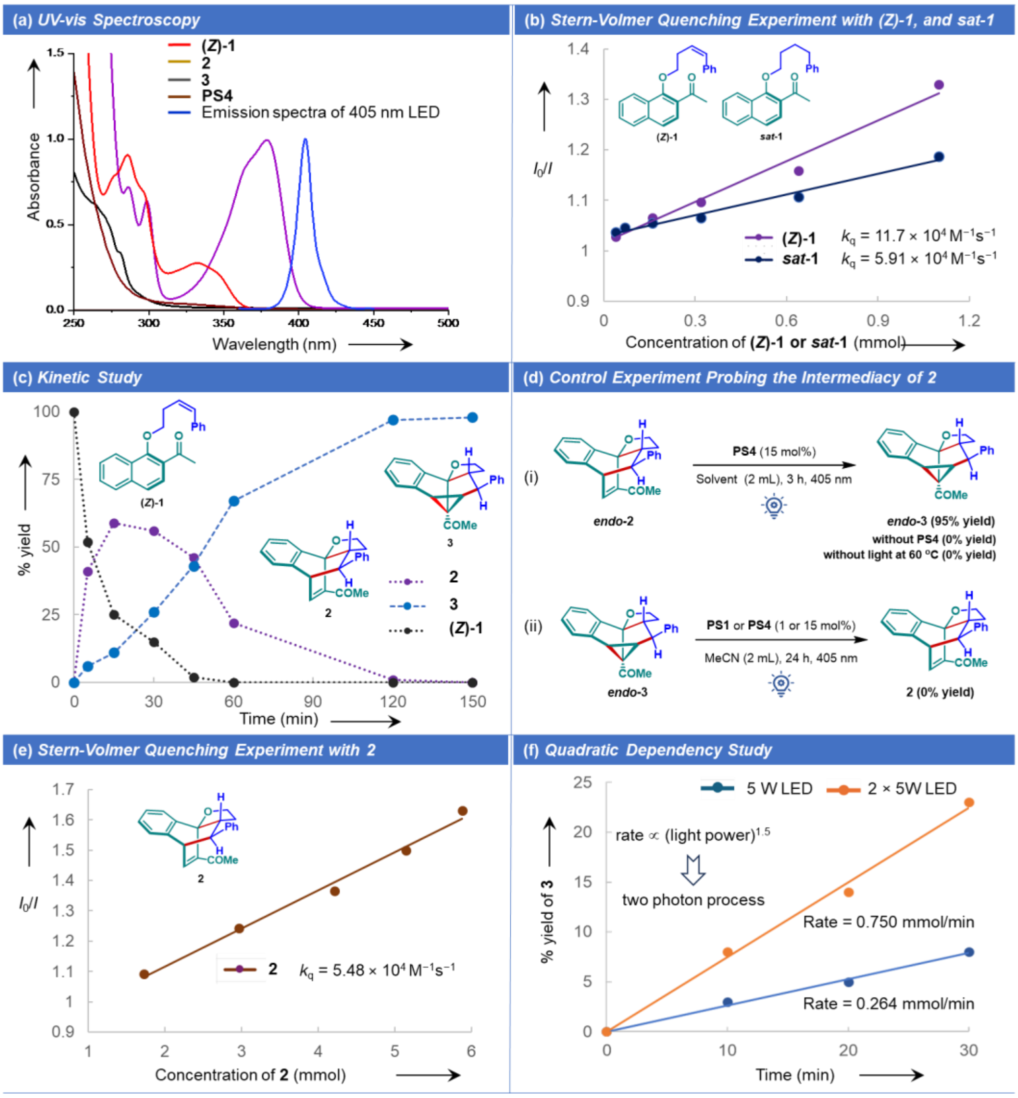

Figure 2: Mechanistic Studies: (a) UV−Vis Spectrum Showing **PS4** as Exclusive Absorbing Species at 405 nm, (b) Stern-Volmer Quenching Studies with **(*Z*)-1** and **sat-1** Highlighting Aromatic Naphthalene Ring as Effective Quencher, (c) Kinetic Monitoring the Reaction to Probe Intermediacy of **2**, (d) Proof of **2** as the Intermediate, and Irreversibility of the Reaction, (e) Triplet Quenching Studies to Probe the

Interaction of **2** with the Excited PS, (f) Quadratic Dependency Study as a Proof for a Two-Photon Process.

We then monitored the kinetics of the ^{VL}EnT cascade reaction (Figure 2c). Initially, we observed rapid consumption of (*Z*)-**1** and the swift formation of the [4 + 2] cycloadduct **2** (after 5 min, conversion of **1** = 48%, **2**:**3** = 41:6). The concentration of **2** peaked and gradually declined as the reaction progressed and completely disappeared after 2 h. The *meta*-cycloadduct was formed at a slower rate. The kinetic profile clearly suggests a two-step consecutive reaction. Heating a solution of [4 + 2] cycloadduct **2** in the dark for 3 h resulted in 93% recovery of **2**, which ruled out the thermal skeleton rearrangement process (Figure 2d, eq. (i)). In comparison, treating the isolated *endo*-[4 + 2] cycloadduct **2** under ^{VL}EnT reaction conditions yielded the desired *meta*-cycloadduct *endo*-**3** in >95% yield (Figure 2d, eq. (i)). These experiments validate the mechanistic hypothesis that **1** initially converts to **2**, which subsequently rearranges to **3** under these conditions. It also suggests that the product selectivity was determined in the initial *para*-cycloaddition step. The cycloadduct **3**, upon irradiation in the presence of **PS4**, did not convert to **2** (Figure 2d, eq. (ii)). This indicated the irreversibility of the process. It presumably is the result of the high E_T (= 70 kcal/mol) of the *meta*-cycloadduct **3** that bypasses the microscopic reversibility of the process, enabling the isolation of the endergonic product **3** as a kinetically trapped species. A luminescence quenching experiment was performed to evaluate the interaction of [4 + 2] cycloadduct **2** with the excited PS (Figure 2e). A quenching constant $k_q = 5.48 \times 10^4\ M^{-1}\ s^{-1}$ signifies efficient interaction of **2** with the excited PS. A 2-fold lower quenching rate compared to **1** could be corroborated with the higher E_T of **2** and a slower formation rate of **3** from **2**.

Accordingly, we postulated that a successive two-photon process operates under the given reaction conditions (Figures 1e and 1f). Substantiating this hypothesis, the quadratic dependency study revealed a 2.84-fold increase in the reaction yield upon doubling the light intensity (Figure 2f). This departure from linearity strongly suggests the potential consumption of two photons in the process.[64] The first photon initiates EnT-mediated [4 + 2] DAC, and then the second photon triggers the rearrangement of the resulting adduct. Additionally, the quantum yield of the reaction was measured to be $\Phi = 0.10$, which eliminates the involvement of a chain reaction (SI S66).

Based on the above observations, a proposed mechanism is depicted in Figure 3a. Furthermore, we have performed DFT calculations at the $SMD_{(MeCN)}$/ωB97X-D/6-311++G**//$SMD_{(MeCN)}$/ωB97X-D/6-31G** level of theory to reveal the dynamic topography traversed during the reaction (Figures 3b, c). The activation-free energy barrier for the thermal concerted *para*-cycloaddition reaction was found to be 37.1 kcal/mol, indicating that it is challenging to achieve at room temperature (Figure S18). Singlet-triplet energy of the photosensitizer, substrate, and cycloadducts at various levels of theory were computed (Table S13). Based on the quenching experiments, the energy transfer from the excited photosensitizer **PS4*** to the ground state of the substrate (Z)-**1** (= ^{1}**A**) to generate an excited state of substrate ^{3}**A** is thermodynamically feasible.

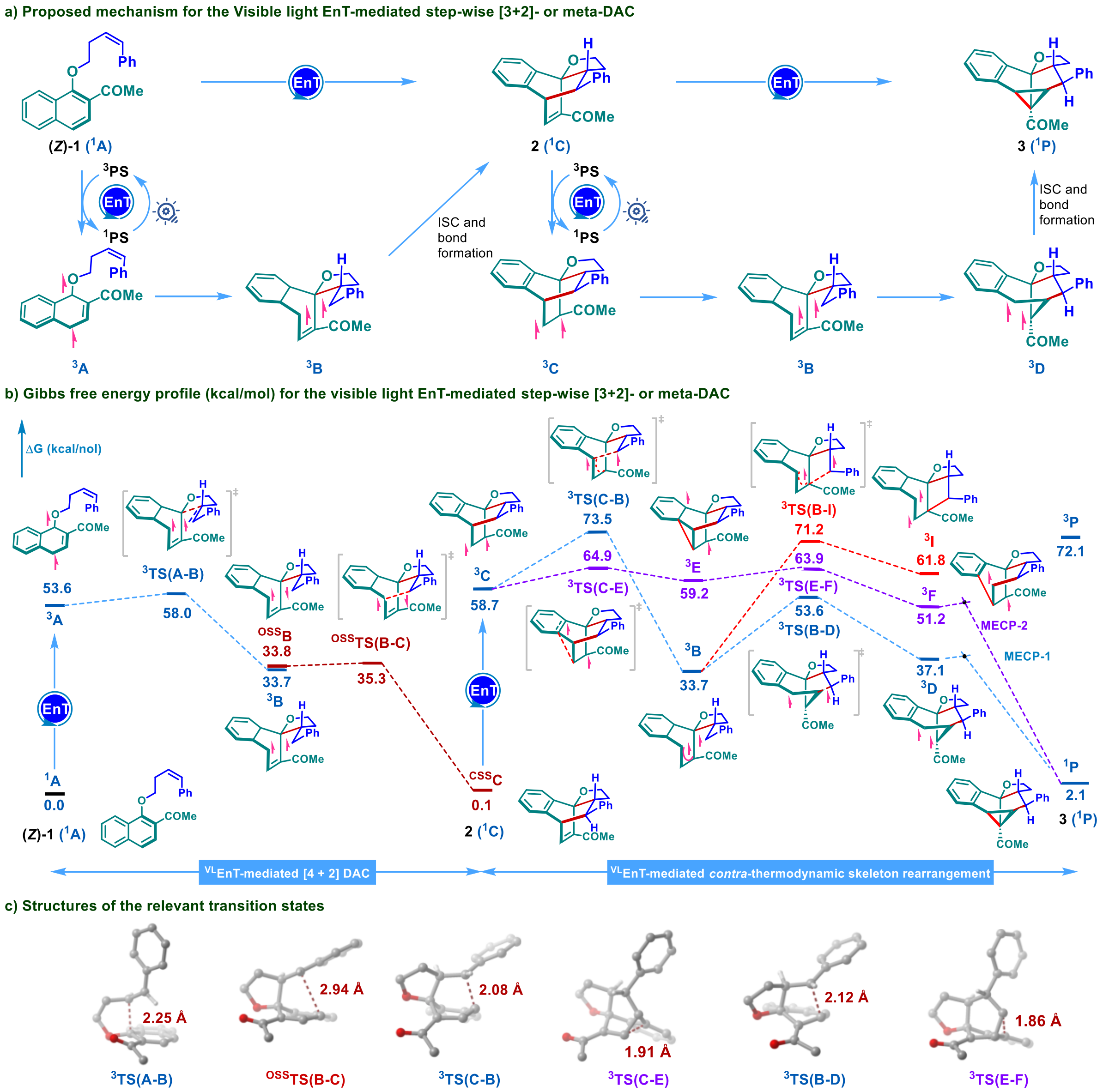

Figure 3: (a) Proposed Mechanism for the Visible-Light EnT-Mediated Stepwise [3+2]- or *meta*-Dearomative Cycloaddition of 2-Acetonaphthalenes, (b) Corresponding Gibbs Free Energy Profile (kcal/mol) Computed on $SMD_{(MeCN)}$/ωB97X-D/6-311++G**//$SMD_{(MeCN)}$/ ωB97X-D/6-31G** Level of Theory. (c) Structures of the Relevant Transition States. OSS = open-shell singlet. Distances between two C-C bonds are mentioned in Angstorm.

In the triplet surface, the ^{3}**A** can intramolecularly form a C–C bond to generate a biradical intermediate ^{3}**B** via ^{3}**TS(A-B)** with a 4.4 kcal/mol barrier and is thermodynamically favorable (ΔΔG° = –19.9 kcal/mol). Notably, the ^{3}**TS(A-B)** represents a crucial transition state that is decisive in determining the major diastereomer. The ^{3}**B** biradical intermediate can undergo C–C bond formation via ^{3}**TS(B-D)**, having an activation-free energy barrier of $\Delta G^{\ddagger}$ = 19.9 kcal/mol, forming the biradical species ^{3}**D**

(Figure 3). This ^{3}**D** species then undergoes inter-system crossing (ISC) and C-C bond formation to yield the product **3** (= ^{1}**P**). However, kinetics and control experiments suggest the intermediacy of the [4 + 2] cycloadduct **2**, in which **2** rearranged to **3** in a successive two-photon process. Computationally, we have found that the triplet biradical species ^{3}**B** can easily undergo ISC to generate open-shell singlet (OSS) biradical species ^{OSS}**B** without a significant thermodynamic loss ($\Delta\Delta G°$ = 0.1 kcal/mol, brown pathway). The selective C–C bond formation on the OSS surface is a highly facile process with a 1.5 kcal/mol barrier to give [4 + 2] cycloadduct **2** (^{1}**C**).

Once ^{1}**C** is formed, it goes to the excited state ^{3}**C** through energy transfer, as experimentally validated by the quenching studies. The rearrangement of triplet biradical ^{3}**C** to ^{3}**B** is a thermodynamically downhill process ($\Delta\Delta G°$ = –25 kcal/mol) and is kinetically favorable with a 14.8 kcal/mol barrier. Now, ^{3}**B** can either follow its path (blue line) to ^{3}**D** or take an alternative route (red line) to generate intermediate ^{3}**I**. The later pathway leading to the [2 + 2] or the *ortho*-cycloadduct required a very high kinetic barrier ($\Delta G^‡$ = 37.5 kcal/mol) via the ^{3}**TS(B-I)**. In comparison, the formation of ^{3}**D** via ^{3}**TS(B-D)** is kinetically feasible. Ultimately, ^{3}**D** undergoes ISC and cyclopropanation to yield the desired product **3** (^{1}**P**) in the singlet surface.

Interestingly, we have found that the reactivity of ^{OSS}**B** and ^{3}**B** are very different in two different spin surfaces, and it is expressed in the difference in regioselectivity in the subsequent bond-forming steps (Figure 4). In ^{OSS}**B**, the highest spin density is at C_{ben}(0.71) and C_{para}(–0.48). As a result, the *para*-cycloadduct **2** (^{1}**C**) is formed preferentially *via* the ^{OSS}**TS(B-C)** in the singlet spin surface (Figures 3b,c). Contrarily, in the ^{3}**B** intermediate, the highest spin density is at C_{ben}(0.75) and C_{meta}(–0.25), and it is translated in the formation of *meta*-cycloadduct **3** (^{1}**P**) *via* the ^{3}**TS(B-D)** and intermediate ^{3}**D** in the triplet spin surface. The observed regioselectivity to the *meta*-product could thus be elucidated.

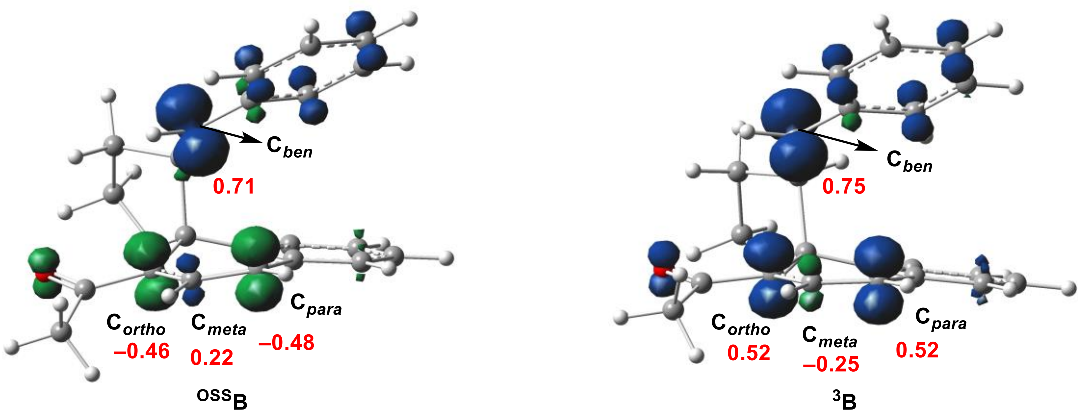

Figure 4: Spin density plot for ^{OSS}**B** and ^{3}**B** intermediates.

We have also computed an alternative pathway involving ^{VL}EnT-mediated di-π methane rearrangement of the *para*-cycloadduct **2** to the *meta*-cycloadduct **3** (Figure 3b, purple line). The ^{VL}EnT-induced 1,2-biradical intermediate ^{3}**C** has the potential to undergo C–C bond formation, leading to the generation of

1,4-biradical species ^{3}**E** via ^{3}**TS(C-E)** with a barrier of 6.2 kcal/mol. From ^{3}**E**, the 1,3-biradical species ^{3}**F** could be generated through ^{3}**TS(E-F)** with a barrier of 4.7 kcal/mol. ^{3}**F** undergoes intersystem crossing (ISC) to form the desired product in the singlet ground surface.

Finally, we began investigating the scope of ^{VL}EnT-induced intramolecular stepwise *meta*-DAC reaction (Scheme 1). A diverse array of electronically biased functional groups, including alkyl, phenyl, di-F, -CF_3, COMe, and CO_2Me, installed at different positions of the aromatic ring at the alkene terminus could be perfectly accommodated. The desired *meta*-cycloadducts **3-9** were isolated with good to excellent 68-93% yields and moderate *endo*-selectivities. Although the diastereoselectivity is suboptimal, the isomers could often be readily distinguished and separated. The intramolecular cascade-cycloaddition with substrates containing heteroaromatic moieties such as pyridine, pyrimidine, and dibenzofuran proceeded to afford the desired products **10-12** in good 76-90% yields. To our satisfaction, complex and biologically important borneol and menthol derivatives of naphthalene tethered alkenes were compatible with the *meta*-DAC reaction. Adducts **13** and **14** were isolated in 69–79% yields. It highlighted the broad functional group compatibility and potential synthetic utility of the protocol.

Next, we aimed to broaden the scope by varying the acyl substituents on the naphthalene skeleton (Scheme 1). To our delight, the different groups like pentyl, cyclobutyl, and cyclohexyl containing acyl-naphthalene derivatives were well tolerated, delivering the products **15-17** in high 71-81% yields and moderate *endo*-selectivities. Moreover, substrate containing β-naphthoates also underwent the proposed *meta*-DAC in a facile manner, and the adducts **18-20** were isolated in high 70-82% yields. The reaction could also be successfully extended to the naphthalene substrates bearing different substituents on the ring. Alkene tethered 6,7-dimethoxy, and 6,7-dimethyl substituted naphthalenes **21**, **22** efficiently gave polycyclic spiroethers in good yields.

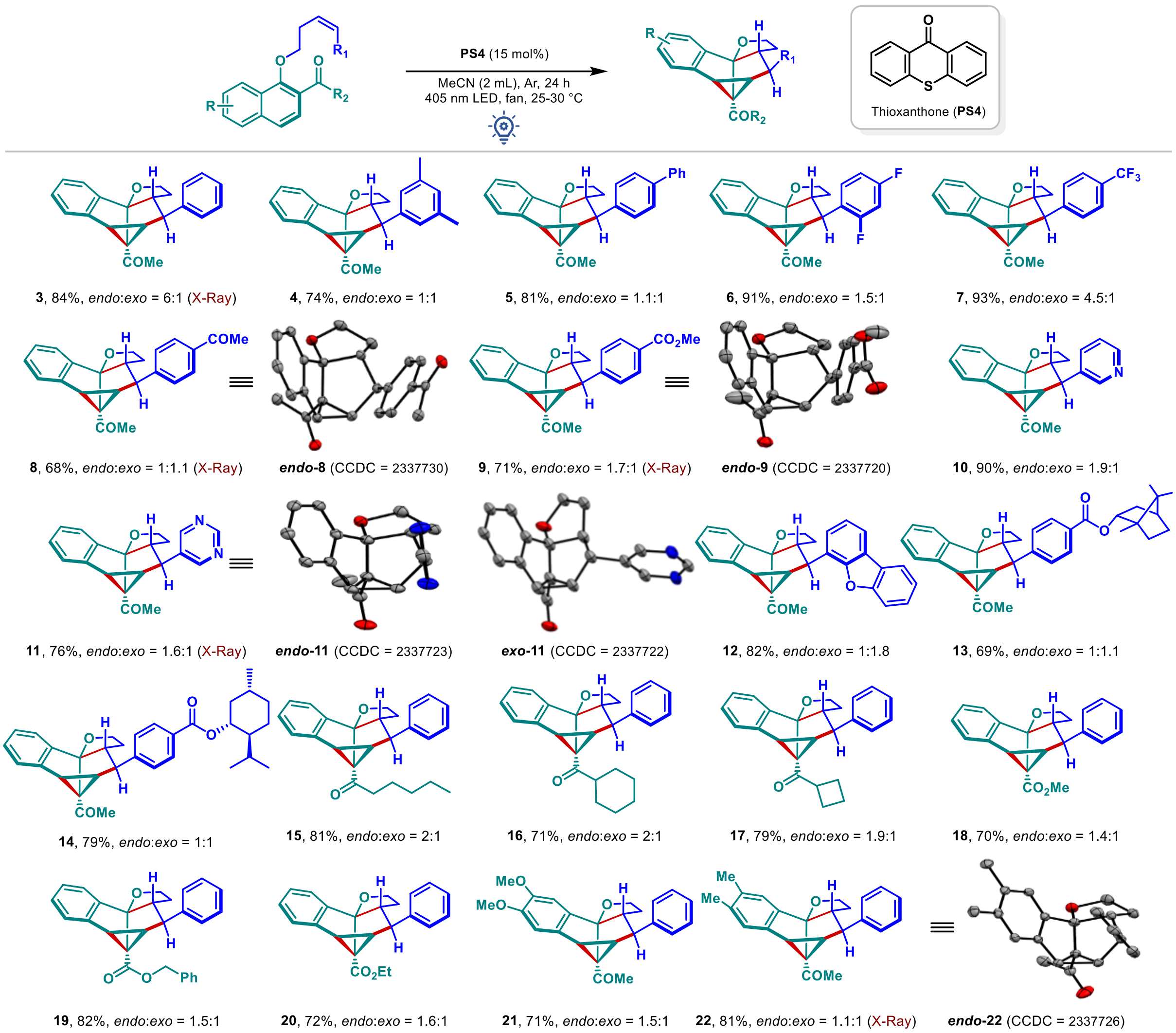

Scheme 1: Substrate Scope of the Visible Light Mediated *meta*-DAC Reaction. Reaction conditions: Reaction was performed on a 0.1 mmol scale in 2 mL MeCN at 25-30 °C under 405 nm Blue LED irradiation under argon. The *endo*/*exo* ratio of products was determined by ^{1}H NMR analysis of the crude reaction mixture using 1,3,5-trimethoxy benzene as an internal standard. Combined yields are given. Isolated yields of each isomers are provided in the Supporting Information. See ref.[58] for crystallographic information.

After establishing the intramolecular visible-light fueled *meta*-DAC, we were keen to explore the intermolecular reaction. Direct irradiation of the mixture of 2-acetyl naphthalene **23** and 1-fluoro-4-vinyl benzene **24** in the presence of **PS-4** under 405 nm LED does not yield *meta*-cycloadduct **25** (SI S69). Pleasingly, a one-pot sequential approach, where **23** and **24** are first irradiated at 427 nm in the presence of **PS-3** followed by 405 nm LED irradiation in the presence of **PS-4**, results in the production of **25** in 21% yield with *exo*:*endo* ratio of 1.3:1 (SI S69). We have recently reported the intermolecular *para*-DAC of naphthalenes with styrenes employing EnT catalysis.[34] Under 405 nm LED irradiation in the presence of **PS-4**, the *para*-cycloadduct **26** (*exo*:*endo* = 2:1), derived from **23** and **24**, transforms

Table 2: *Contra*-Thermodynamic Skeleton Rearrangement of *para*-Cycloadduct to the *meta*-Cycloadduct via Visible Light Fuelled EnT Catalysis.[a]

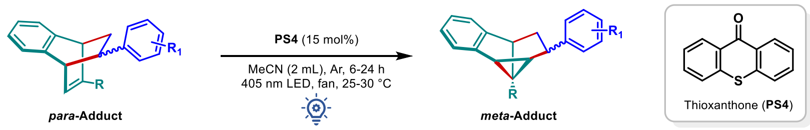

entry	*para*-Adduct	*meta*-Adduct	% yield of *meta*-Adduct	entry	*para*-Adduct	*meta*-Adduct	% yield of *meta*-Adduct
1	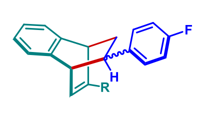 **26**, *endo*:*exo* = 2:1	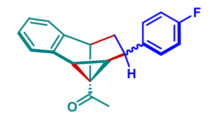 **25**	48% *endo*:*exo* = 1.3:1 6h	8	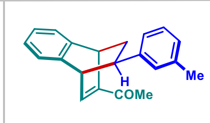 *endo*-**31**	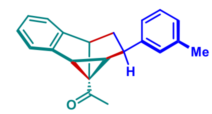 *endo*-**32**	42% *endo*:*exo* > 20:1 5h
2	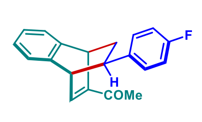 *endo*-**26**	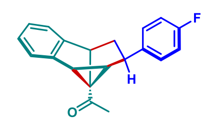 *endo*-**25**	48% *endo*:*exo* > 20:1 6h	9	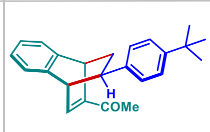 *endo*-**33**	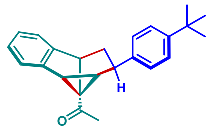 *endo*-**34**	54% *endo*:*exo* > 20:1 24h
3	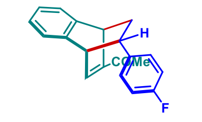 *exo*-**26**	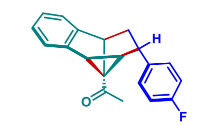 *exo*-**25**	45% *endo*:*exo* < 1:20 6h	10	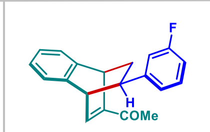 *endo*-**35**	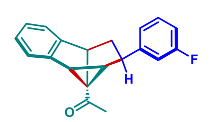 *endo*-**36**	71% *endo*:*exo* > 20:1 6h
4	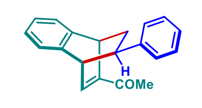 *endo*-**27**	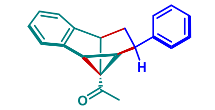 *endo*-**28**	50% *endo*:*exo* > 20:1 5h	11	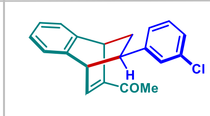 *endo*-**37**	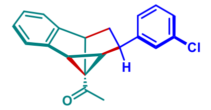 *endo*-**38**	74% *endo*:*exo* > 20:1 24h
5	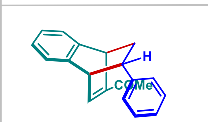 *exo*-**27**	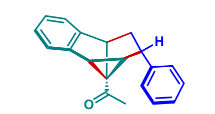 *exo*-**28**	56% *endo*:*exo* < 1:20 18h	12	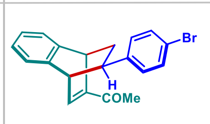 *endo*-**39**	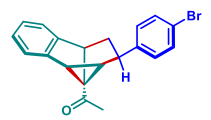 *endo*-**40**	57% *endo*:*exo* > 20:1 24h
6	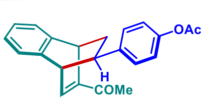 *endo*-**29**	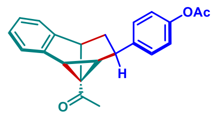 *endo*-**30**	70% *endo*:*exo* > 20:1 24h	13	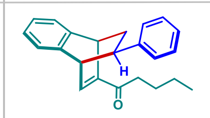 *endo*-**41**	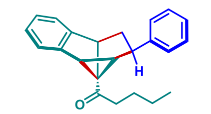 *endo*-**42**	50% *endo*:*exo* > 20:1 18h
7	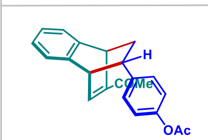 *exo*-**29**	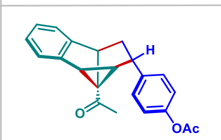 *exo*-**30**	56% *endo*:*exo* < 1:20 24h	14	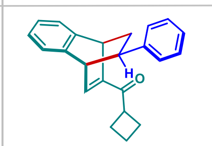 *endo*-**43**	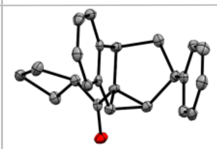 *endo*-**44** (CCDC = 2337729)	67% *endo*:*exo* > 20:1 18h

[a]Reaction condition: Reaction was performed on a 0.1 mmol scale in 2 mL MeCN at 25-30 °C under 405 nm Blue LED irradiation under argon. The *endo*/*exo* ratio of products was determined by ^{1}H NMR analysis of the crude reaction mixture using 1,3,5-trimethoxy benzene as an internal standard. Isolated yields are given. See ref.[58] for crystallographic information.

into the *meta*-cycloadduct **25** in 48% yield (*exo*:*endo* = 1.3:1, Table 2, entry 1). Furthermore, we have found that the **PS-4**-catalyzed rearrangement of *para*-cycloadduct is stereospecific. The irradiation of *endo*-**26** in the presence of **PS-4** produced the *endo*-diastereoisomer of the *meta*-cycloadduct **25** in 48% yield (Table 2, entry 2), and the *exo*-**26** delivered the *exo*-**25** in 45% yield (entry 3). The chemistry could thus be ideal for discovery purposes, where generating multiple diastereomers allows for a comprehensive evaluation of chemical space. To our delight, the reaction accommodates a large scope, and both diastereomers could be selectively obtained from the corresponding *para*-cycloadducts (entries 4-12). Substrate-bearing diverse electronically biased groups in the phenyl ring delivered the desired products in 42-70% of yields. Besides the acetyl group, the substrate-bearing long-chain pentyl and cyclobutyl groups also underwent the reaction smoothly (entries 13-14). Notably, we observed only a single diastereomer in all the cases.

Next, we explored the possibility of derivatization of the isolated cycloadduct (Scheme 3). The *m*-CPBA mediated Bayer-Villiger oxidation of *endo*-**3** produced the acetate **45** in 77% yield. To our relish, we were able to perform lithium aluminium hydride-mediated reduction of the acetyl group on the compounds *endo*-**3** and *endo*-**28** to generate the secondary alcohols **46** and **47** in excellent 82% and 54% yields with 3:1 and 2.5:1 d.r., respectively with the retention of highly-strained cyclopropane ring. Further, **47** could be reacted with the anti-inflammatory drug oxaprozin **48** to produce the corresponding oxaprozin derivative **49** in good yield. Subjecting compound *endo*-**8** and *endo*-**23** to HBr in acetone at 45 °C for 24 hours led to the selective hydrobromination of the cyclopropane ring *via* its ring-opening to give the products containing intricate bicyclo[3.2.1]octane rings **50** and **51** in 62% and 51% yields, respectively. Finally, the treatment of *endo*-**3** with hydrogen (1 atm) in the presence of Pd-C led to selective hydrogenolysis of the cyclopropane ring, yielding angular oxy-triquinane framework **52** in 58% yield as a single diastereomer.

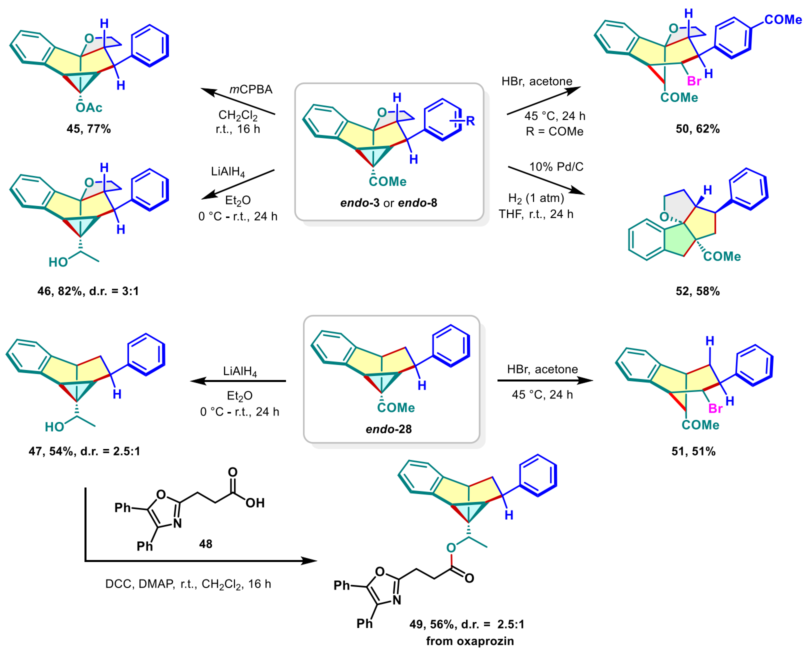

Scheme 3: Post-synthetic application of [3 + 2] cycloaddition products.

Conclusion

In this study, we present a formal dearomative *meta*-cycloaddition of 2-acetonaphthalenes achieved through a two-step visible light-mediated triplet-triplet energy transfer (^{VL}EnT), which avoids the need to reach energetically higher singlet excited states. Our approach involved carefully selecting a photosensitizer and reaction conditions, guided by thorough literature surveys and DFT calculations, to selectively facilitate the contra-thermodynamic stepwise [4 + 2] dearomative cycloaddition and subsequent skeletal rearrangement cascade. Comprehensive DFT studies and electrochemical, photoluminescence, kinetic, quadratic dependency, and control experiments provide robust support for the ^{VL}EnT cascade mechanism. The developed protocol enables the synthesis of highly sp3-rich polycyclic frameworks in high yields with moderate endo-selectivities and broad functional group compatibility. Moreover, integrating bioactive agents and facilitating a diverse array of post-synthetic derivatizations further underscore the efficiency and applicability of the developed protocol. Further studies to unravel apt systems bearing latent potential to undergo cycloadditions under visible light irradiation are in progress in our laboratory.

Author Contributions

All authors have given approval to the final version of the paper.

Data availability

The supplementary information includes all experimental details, including optimization of the synthetic method, synthesis and characterization of all starting materials and products reported in this study, mechanistic studies, NMR spectra of all products, crystallographic data, and computational studies.

Funding

DST-SERB, GoI (grant no. CRG/2023/004175, SPG/2021/0043445)

Notes

The authors declare no competing financial interest.

Acknowledgments

The BM thanks DST-SERB, GoI (grant no. CRG/2023/004175), and GJ thanks DST-SERB, GoI (grant no. SPG/2021/0043445) for financial support. PR thanks INSPIRE, SN thanks PMRF, and KG thanks CSIR for fellowships.

References

1. Newhouse, T.; Baran, P. S.; Hoffmann, R. W., The economies of synthesis. *Chem. Soc. Rev.* **2009**, *38*, 3010-3021.
2. Nicolaou, K. C.; Rigol, S., Perspectives from nearly five decades of total synthesis of natural products and their analogues for biology and medicine. *Nat. Prod. Rep.* **2020**, *37*, 1404-1435.

3. Clemente, D. B.; Coelho, J. A. S., A Historical Review of the Total Synthesis of Natural Products Developed in Portugal. *Eur. J. Org. Chem.* **2023**, *26*, e202300193.
4. Walji, A. M.; MacMillan, D. W. C., Strategies to bypass the taxol problem. Enantioselective cascade catalysis, a new approach for the efficient construction of molecular complexity. *Synlett* **2007**, *2007*, 1477-1489.
5. Nicolaou, K. C.; Chen, J. S., The art of total synthesis through cascade reactions. *Chem. Soc. Rev.* **2009**, *38*, 2993-3009.
6. Grondal, C.; Jeanty, M.; Enders, D., Organocatalytic cascade reactions as a new tool in total synthesis. *Nat. Chem.* **2010**, *2*, 167-178.
7. Remy, R.; Bochet, C. G., Arene–Alkene Cycloaddition. *Chem. Rev.* **2016**, *116*, 9816-9849.
8. Roche, S. P.; Porco Jr., J. A., Dearomatization Strategies in the Synthesis of Complex Natural Products. *Angew. Chem. Int. Ed.* **2011**, *50*, 4068-4093.
9. Peng, L.; Zeng, Z.; Li, K.; Liu, Y.; Lan, Y.; Yan, H., Regiodivergent catalytic asymmetric dearomative cycloaddition of bicyclic heteroaromatics. *Sci. Adv.* **2023**, *9*, eadg1645.
10. Hao, E.-J.; Fu, D.-D.; Wang, D.-C.; Zhang, T.; Qu, G.-R.; Li, G.-X.; Lan, Y.; Guo, H.-M., Chemoselective asymmetric dearomative [3 + 2] cycloaddition reactions of purines with aminocyclopropanes. *Org. Chem. Front.* **2019**, *6*, 863-867.
11. Gall, B. K.; Smith, A. K.; Ferreira, E. M., Dearomative (3+2) Cycloadditions between Indoles and Vinyldiazo Species Enabled by a Red-Shifted Chromium Photocatalyst. *Angew. Chem. Int. Ed.* **2022**, *61*, e202212187.
12. Ryckaert, B.; Hullaert, J.; Van Hecke, K.; Winne, J. M., Dearomative (3 + 2) Cycloadditions of Unprotected Indoles. *Org. Lett.* **2022**, *24*, 4119-4123.
13. James, M. J.; Schwarz, J. L.; Strieth-Kalthoff, F.; Wibbeling, B.; Glorius, F., Dearomative Cascade Photocatalysis: Divergent Synthesis through Catalyst Selective Energy Transfer. *J. Am. Chem. Soc.* **2018**, *140*, 8624-8628.
14. Zhu, M.; Zheng, C.; Zhang, X.; You, S.-L., Synthesis of Cyclobutane-Fused Angular Tetracyclic Spiroindolines via Visible-Light-Promoted Intramolecular Dearomatization of Indole Derivatives. *J. Am. Chem. Soc.* **2019**, *141*, 2636-2644.
15. Martynova, E. A.; Voloshkin, V. A.; Guillet, S. G.; Bru, F.; Beliš, M.; Van Hecke, K.; Cazin, C. S. J.; Nolan, S. P., Energy transfer (EnT) photocatalysis enabled by gold-N-heterocyclic carbene (NHC) complexes. *Chem. Sci.* **2022**, *13*, 6852-6857.
16. Zhu, M.; Zhang, X.; Zheng, C.; You, S.-L., Visible-Light-Induced Dearomatization via [2+2] Cycloaddition or 1,5-Hydrogen Atom Transfer: Divergent Reaction Pathways of Transient Diradicals. *ACS Catal.* **2020**, *10*, 12618-12626.
17. Zhu, M.; Huang, X.-L.; Xu, H.; Zhang, X.; Zheng, C.; You, S.-L., Visible-Light-Mediated Synthesis of Cyclobutene-Fused Indolizidines and Related Structural Analogs. *Chinese J. Org. Chem.* **2021**, *3*, 652-664.
18. Oderinde, M. S.; Mao, E.; Ramirez, A.; Pawluczyk, J.; Jorge, C.; Cornelius, L. A. M.; Kempson, J.; Vetrichelvan, M.; Pitchai, M.; Gupta, A.; Gupta, A. K.; Meanwell, N. A.; Mathur, A.; Dhar, T. G. M., Synthesis of Cyclobutane-Fused Tetracyclic Scaffolds via Visible-Light Photocatalysis for Building Molecular Complexity. *J. Am. Chem. Soc.* **2020**, *142*, 3094-3103.
19. Sauvé, E. R.; Mayder, D. M.; Kamal, S.; Oderinde, M. S.; Hudson, Z. M., An imidazoacridine-based TADF material as an effective organic photosensitizer for visible-light-promoted [2 + 2] cycloaddition. *Chem. Sci.* **2022**, *13*, 2296-2302.
20. Rolka, A. B.; Koenig, B., Dearomative Cycloadditions Utilizing an Organic Photosensitizer: An Alternative to Iridium Catalysis. *Org. Lett.* **2020**, *22*, 5035-5040.

21. Proessdorf, J.; Jandl, C.; Pickl, T.; Bach, T., Arene Activation through Iminium Ions: Product Diversity from Intramolecular Photocycloaddition Reactions. *Angew. Chem. Int. Ed.* **2022**, *61*, e202208329.
22. Hu, N.; Jung, H.; Zheng, Y.; Lee, J.; Zhang, L.; Ullah, Z.; Xie, X.; Harms, K.; Baik, M.-H.; Meggers, E., Catalytic Asymmetric Dearomatization by Visible-Light-Activated [2+2] Photocycloaddition. *Angew. Chem. Int. Ed.* **2018**, *57*, 6242-6246.
23. Oderinde, M. S.; Ramirez, A.; Dhar, T. G. M.; Cornelius, L. A. M.; Jorge, C.; Aulakh, D.; Sandhu, B.; Pawluczyk, J.; Sarjeant, A. A.; Meanwell, N. A.; Mathur, A.; Kempson, J., Photocatalytic Dearomative Intermolecular [2 + 2] Cycloaddition of Heterocycles for Building Molecular Complexity. *J. Org. Chem.* **2021**, *86*, 1730-1747.
24. Kleinmans, R.; Dutta, S.; Ozols, K.; Shao, H.; Schäfer, F.; Thielemann, R. E.; Chan, H. T.; Daniliuc, C. G.; Houk, K. N.; Glorius, F., ortho-Selective Dearomative [2π + 2σ] Photocycloadditions of Bicyclic Aza-Arenes. *J. Am. Chem. Soc.* **2023**, *145*, 12324-12332.
25. Bellotti, P.; Rogge, T.; Paulus, F.; Laskar, R.; Rendel, N.; Ma, J.; Houk, K. N.; Glorius, F., Visible-Light Photocatalyzed peri-(3 + 2) Cycloadditions of Quinolines. *J. Am. Chem. Soc.* **2022**, *144*, 15662-15671.
26. Lee, W.; Koo, Y.; Jung, H.; Chang, S.; Hong, S., Energy-transfer-induced [3+2] cycloadditions of N–N pyridinium ylides. *Nat. Chem.* **2023**, *15*, 1091-1099.
27. Ma, J.; Strieth-Kalthoff, F.; Dalton, T.; Freitag, M.; Schwarz, J. L.; Bergander, K.; Daniliuc, C.; Glorius, F., Direct Dearomatization of Pyridines via an Energy-Transfer-Catalyzed Intramolecular [4+2] Cycloaddition. *Chem* **2019**, *5*, 2854-2864.
28. Zhu, M.; Xu, H.; Zhang, X.; Zheng, C.; You, S.-L., Visible-Light-Induced Intramolecular Double Dearomative Cycloaddition of Arenes. *Angew. Chem. Int. Ed.* **2021**, *60*, 7036-7040.
29. Chiminelli, M.; Serafino, A.; Ruggeri, D.; Marchiò, L.; Bigi, F.; Maggi, R.; Malacria, M.; Maestri, G., Visible-Light Promoted Intramolecular para-Cycloadditions on Simple Aromatics. *Angew. Chem. Int. Ed.* **2023**, *62*, e202216817.
30. Ma, J.; Chen, S.; Bellotti, P.; Guo, R.; Schäfer, F.; Heusler, A.; Zhang, X.; Daniliuc, C.; Brown, M. K.; Houk, K. N.; Glorius, F., Photochemical intermolecular dearomative cycloaddition of bicyclic azaarenes with alkenes. *Science* **2021**, *371*, 1338-1345.
31. Morofuji, T.; Nagai, S.; Chitose, Y.; Abe, M.; Kano, N., Protonation-Enhanced Reactivity of Triplet State in Dearomative Photocycloaddition of Quinolines to Olefins. *Org. Lett.* **2021**, *23*, 6257-6261.
32. Guo, R.; Adak, S.; Bellotti, P.; Gao, X.; Smith, W. W.; Le, S. N.; Ma, J.; Houk, K. N.; Glorius, F.; Chen, S.; Brown, M. K., Photochemical Dearomative Cycloadditions of Quinolines and Alkenes: Scope and Mechanism Studies. *J. Am. Chem. Soc.* **2022**, *144*, 17680-17691.
33. Bhakat, M.; Khatua, B.; Biswas, P.; Guin, J., Brønsted Acid-Promoted Intermolecular Dearomative Photocycloaddition of Bicyclic Azaarenes with Olefins under Aerobic Conditions. *Org. Lett.* **2023**, *25*, 3089-3093.
34. Rai, P.; Maji, K.; Jana, S. K.; Maji, B., Intermolecular dearomative [4 + 2] cycloaddition of naphthalenes via visible-light energy-transfer-catalysis. *Chem. Sci.* **2022**, *13*, 12503-12510.
35. Wang, W.; Cai, Y.; Guo, R.; Brown, M. K., Synthesis of complex bicyclic scaffolds by intermolecular photosensitized dearomative cycloadditions of activated alkenes and naphthalenes. *Chem. Sci.* **2022**, *13*, 13582-13587.
36. Donati, D.; Fusi, S.; Ponticelli, F., Photocycloaddition on 2-methyloxazolo[5,4-b]pyridine: a route to the oxazolo[5,4-b]azocine system. *Tetrahedron Lett.* **1996**, *37*, 5783-5786.
37. Sakamoto, M.; Sano, T.; Takahashi, M.; Yamaguchi, K.; Fujita, T.; Watanabe, S., Photochemistry of heteroaromatics–a novel photocycloaddition of 2-alkoxy-3-cyanopyridines with methacrylonitrile. *Chem. Commun.* **1996**, 1349-1350.

38. Kishikawa, K.; Akimoto, S.; Kohmoto, S.; Yamamoto, M.; Yamada, K., Intramolecular photo[4+2]cycloaddition of an enone with a benzene ring. *J. Chem. Soc., Perkin Trans. 1* **1997**, 77-84.
39. Strieth-Kalthoff, F.; Glorius, F., Triplet Energy Transfer Photocatalysis: Unlocking the Next Level. *Chem* **2020**, *6*, 1888-1903.
40. Zhu, M.; Zhang, X.; Zheng, C.; You, S.-L., Energy-Transfer-Enabled Dearomative Cycloaddition Reactions of Indoles/Pyrroles via Excited-State Aromatics. *Acc. Chem. Res.* **2022**, *55*, 2510-2525.
41. Strieth-Kalthoff, F.; Henkel, C.; Teders, M.; Kahnt, A.; Knolle, W.; Gómez-Suárez, A.; Dirian, K.; Alex, W.; Bergander, K.; Daniliuc, C. G.; Abel, B.; Guldi, D. M.; Glorius, F., Discovery of Unforeseen Energy-Transfer-Based Transformations Using a Combined Screening Approach. *Chem* **2019**, *5*, 2183-2194.
42. Zhen, G.; Zeng, G.; Jiang, K.; Wang, F.; Cao, X.; Yin, B., Visible-Light-Induced Diradical-Mediated ipso-Cyclization towards Double Dearomative [2+2]-Cycloaddition or Smiles-Type Rearrangement. *Chem. Eur. J.* **2023**, *29*, e202203217.
43. Becker, M. R.; Richardson, A. D.; Schindler, C. S., Functionalized azetidines via visible light-enabled aza Paternò-Büchi reactions. *Nat. Commun.* **2019**, *10*, 5095.
44. Becker, M. R.; Wearing, E. R.; Schindler, C. S., Synthesis of azetidines via visible-light-mediated intermolecular [2+2] photocycloadditions. *Nat. Chem.* **2020**, *12*, 898-905.
45. Zhang, Z.; Yi, D.; Zhang, M.; Wei, J.; Lu, J.; Yang, L.; Wang, J.; Hao, N.; Pan, X.; Zhang, S.; Wei, S.; Fu, Q., Photocatalytic Intramolecular [2 + 2] Cycloaddition of Indole Derivatives via Energy Transfer: A Method for Late-Stage Skeletal Transformation. *ACS Catal.* **2020**, *10*, 10149-10156.
46. Bryce-Smith, D., Orbital symmetry relationships for thermal and photochemical concerted cycloadditions to the benzene ring. *J. Chem. Soc. D* **1969**, 806-808.
47. Ferree Jr, W.; Grutzner, J. B.; Morrison, H., Organic photochemistry. XV. Photochemistry of bichromophoric molecules. Intramolecular cycloaddition and cis-trans isomerization of 6-phenyl-2-hexene in solution. *J. Am. Chem. Soc.* **1971**, *93*, 5502-5512.
48. Arns, S.; Barriault, L., Concise Synthesis of the neo-Clerodane Skeleton of Teucrolivin A Using a Pericyclic Reaction Cascade. *J. Org. Chem.* **2006**, *71*, 1809-1816.
49. Opatz, T.; Kolshorn, H.; Birnbacher, J.; Schüffler, A.; Deininger, F.; Anke, T., The Creolophins: A Family of Linear Triquinanes from Creolophus cirrhatus (Basidiomycete). *Eur. J. Org. Chem.* **2007**, *2007*, 5546-5550.
50. Zhang, Y.; Di, Y.; He, H.; Li, S.; Lu, Y.; Gong, N.; Hao, X., Daphmalenines A and B: Two New Alkaloids with Unusual Skeletons from Daphniphyllum himalense. *Eur. J. Org. Chem.* **2011**, *2011*, 4103-4107.
51. Zhang, F.; Zhang, C.-R.; Tao, X.; Wang, J.; Chen, W.-S.; Yue, J.-M., Phragmalin-type limonoids with NF-κB inhibition from Chukrasia tabularis var. velutina. *Bioorganic Med. Chem. Lett.* **2014**, *24*, 3791-3796.
52. Lankri, D.; Mostinski, Y.; Tsvelikhovsky, D., Palladium-Catalyzed Cascade Assembly of Tricyclic Spiroethers from Diene-Alcohol Precursors. *J. Org. Chem.* **2017**, *82*, 9452-9463.
53. King, T. J.; Farrell, I. W.; Halsall, T. G.; Thaller, V., Alliacolide, a new bicyclic sesquiterpene epoxy-lactone with a novel carbon skeleton from cultures of the fungus Marasmius alliaceus(Jacques ex Fr.)Fr; X-ray structure. *J. Chem. Soc., Chem. Commun.* **1977**, 727-728.
54. Farrell, I. W.; Halsall, T. G.; Thaller, V.; Bradshaw, A. P. W.; Hanson, J. R., Structures of some new sesquiterpenoid metabolites of Marasmius alliaceus. *J. Chem. Soc., Perkin Trans.* **1981**, 1790-1793.
55. Koshikawa, T.; Nagashima, Y.; Tanaka, K., Gold-Catalyzed [3 + 2] Annulation, Carbenoid Transfer, and C–H Insertion Cascade: Elucidation of Annulation Mechanisms via Benzopyrylium Intermediates. *ACS Catal.* **2021**, *11*, 1932-1937.

56. Huang, H.-M.; McDouall, J. J. W.; Procter, D. J., SmI2-catalysed cyclization cascades by radical relay. *Nat. Catal.* **2019**, *2*, 211-218.
57. Verdugo, F.; da Concepción, E.; Rodiño, R.; Calvelo, M.; Mascareñas, J. L.; López, F., Pd-Catalyzed (3 + 2) Heterocycloadditions between Alkylidenecyclopropanes and Carbonyls: Straightforward Assembly of Highly Substituted Tetrahydrofurans. *ACS Catal.* **2020**, *10*, 7710-7718.
58. CCDC-2337727 (*endo*-3), CCDC-2337728 (*exo*-3), CCDC-2337730 (*endo*-8), CCDC-2337720 (*endo*-9), CCDC-2337723 (*endo*-11), CCDC-2337722 (*exo*-11), CCDC-2337726 (*endo*-22), CCDC-2337729 (*endo*-44) contain the supplementary crystallographic data.
59. Yan, P.; Stegbauer, S.; Wu, Q.; Kolodzeiski, E.; Stein, C. J.; Lu, P.; Bach, T., Enantioselective Intramolecular ortho Photocycloaddition Reactions of 2-Acetonaphthones. *Angew. Chem. Int. Ed. n/a*, e202318126.
60. Zhu, M.; Gao, Y.-J.; Huang, X.-L.; Li, M.; Zheng, C.; You, S.-L., Photo-induced intramolecular dearomative [5 + 4] cycloaddition of arenes for the construction of highly strained medium-sized-rings. *Nat. Commun.* **2024**, *15*, 2462.
61. Zhang, X.; Rovis, T., Photocatalyzed Triplet Sensitization of Oximes Using Visible Light Provides a Route to Nonclassical Beckmann Rearrangement Products. *J. Am. Chem. Soc.* **2021**, *143*, 21211-21217.
62. Romero, N. A.; Nicewicz, D. A., Organic Photoredox Catalysis. *Chem. Rev.* **2016**, *116*, 10075-10166.
63. Kim, D.; Teets, T. S., Strategies for accessing photosensitizers with extreme redox potentials. *Chem. Phys. Rev.* **2022**, *3*, 021302.
64. Glaser, F.; Kerzig, C.; Wenger, O. S., Multi-Photon Excitation in Photoredox Catalysis: Concepts, Applications, Methods. *Angew. Chem. Int. Ed.* **2020**, *59*, 10266-10284.